THE STUDY ON ESTABLISHING THE EXPERIMENTAL DEPENDENCE OF THE COMPRESSED ZONE RADIUS AND THE OBSERVED HEIGHT OF THE SPLASHED FUNNEL IN THE CLAY MEDIUM UNDER WATER

Dam Trong Thang[1,*], Vu Tung Lam[1], To Duc Tho[2]

[1]*Le Quy Don Technical University;* [2]*Military Science Bureau*

Abstract

Currently, there has not been the general formula calculating the radius of the compressed zone and the observed height of the explosive funnel destroying the ground under water. Therefore, this paper used experiment results from the previous study related to the clay medium under water. This paper studied and established a multivariable regression model, finding the general experiment law relating to the dependence relation between the radius of the compressed zone and the observed height of the splashed funnel in the clay medium under water and the water depth, the depth of buried explosive charge in the clay medium and the radius of explosive charges. The model is built with python programming language version 3. The law of model is evaluated and compared to actual values in experiments through the coefficient of determination R^2. The result showed that the chosen law reached the relatively high accuracy.

Keywords: *Blasting; underwater blasting; blasting in clay medium; splashed explosion; compressed explosion; machine learning; regression.*

1. Introduction

Currently, in the field of blasting works, the general theory system and the calculation of blasting plans have just only resolved explosion missions on land. The calculation system of explosions destroying rock under water has mainly followed the way of inheriting the terrestrial explosion method, there has not been a general calculation method for parameters of the explosion, underwater blasting depends on the water height [1, 2, 4, 12, 13, 15]. Hence, it is an essential studying direction for studying the experiment law of the dependence between a side which includes the radius of the compressed zone and the observed height of the splashed funnel, and another side which includes the depth of buried explosives, the water depth and the radius of explosive charges. This studying direction also contains scientific and practical meanings.

Establishing experiment laws on relations among parameters at multidimensional and multivariable level found it hard to give a general, successive form from splashed explosions to smoldered explosions with the traditional regression method [2].

[*] Email: thangdt@lqdtu.edu.vn

https://doi.org/10.56651/lqdtu.jst.v3.n02.157.sce

Currently, achievements in the field of artificial intelligence have been being applied successfully in all scientific and technical branches. In particular, machine learning and deep learning are efficient approaches when it comes to the field of data science. Hence, this paper concentrates on establishing a regression model based on machine learning algorithms, finding the dependence law of the radius of the compressed zone, the observed height of the splashed funnel on the depth of buried explosives in clay, the water depth and the radius of explosive charges.

2. Analyzing results of the experiment study

Based on the experiment study on diminished model with explosive charges 0.5 g (Ten) in clay medium under water, the authors gave similarity laws about the dependence of the radius of the compressed zone and the observed height of the splashed funnel in clay medium under water as follows [3]:

* When the depth of buried explosive charges in clay *W/r* = 1:

$$\frac{R_K}{r} = -0.0199\left(\frac{h}{r}\right)^2 + 0.5819\left(\frac{h}{r}\right) + 12.732\ ,\ R^2 = 0.9791,\ \text{at}\ 0 \le \frac{h}{r} \le 36; \quad (1)$$

$$\frac{R_K}{r} = \frac{R_{K_{bh}}}{r} = 8\ ,\ \Delta = 0\%,\ \text{at}\ 36 \le \frac{h}{r} \le 60; \quad (2)$$

$$\frac{P}{r} = -0.0083\left(\frac{h}{r}\right)^2 + 0.4082\left(\frac{h}{r}\right) + 18.797,\ R^2 = 0.7222,\ \text{at}\ 0 \le \frac{h}{r} \le 60. \quad (3)$$

* When the depth of buried explosive charges in clay *W/r* = 3:

$$\frac{R_K}{r} = 12.762.e^{-0.015.\frac{h}{r}}\ ,\ R^2 = 0.9827,\ \text{at}\ 0 \le \frac{h}{r} \le 36; \quad (4)$$

$$\frac{R_K}{r} = \frac{R_{K_{bh}}}{r} \approx 7.5\ ,\ \Delta = \pm 7\%,\ \text{at}\ 36 \le \frac{h}{r} \le 70; \quad (5)$$

$$\frac{P}{r} = -0.005\left(\frac{h}{r}\right)^2 + 0.2913\left(\frac{h}{r}\right) + 21.445\ ,\ R^2 = 0.7056,\ \text{at}\ 0 \le \frac{h}{r} \le 70. \quad (6)$$

* When the depth of buried explosive charges in clay *W/r* = 7:

$$\frac{R_K}{r} = 12.212.e^{-0.017.\frac{h}{r}},\ R^2 = 0.8457,\ \text{at}\ 0 \le \frac{h}{r} \le 24; \quad (7)$$

$$\frac{R_K}{r} = \frac{R_{K_{bh}}}{r} \approx 8\ ,\ \Delta = \pm 13\%,\ \text{at}\ 24 \le \frac{h}{r} \le 60; \quad (8)$$

$$\frac{P}{r} = -0.0133\left(\frac{h}{r}\right)^2 + 0.744\left(\frac{h}{r}\right) + 24.922,\ R^2 = 0.946,\ \text{at}\ 0 \le \frac{h}{r} \le 60. \quad (9)$$

* When the depth of buried explosive charges in clay *W/r* = 11:

$$\frac{R_K}{r} = 14.602.e^{-0.074.\frac{h}{r}}\ ,\ R^2 = 0.9983,\ \text{at}\ 0 \le \frac{h}{r} \le 8; \quad (10)$$

$$\frac{R_K}{r} = \frac{R_{K_{bh}}}{r} \approx 8,\ \Delta = 0\%,\ \text{at}\ 8 \le \frac{h}{r} \le 24; \tag{11}$$

$$\frac{P}{r} = -0.0155\left(\frac{h}{r}\right)^2 + 0.5217\left(\frac{h}{r}\right) + 28.223,\ R^2 = 0.7124,\ \text{at}\ 0 \le \frac{h}{r} \le 24. \tag{12}$$

where R_K is the radius of the compressed zone; $R_{K_{bh}}$ is the radius of the compressed zone when saturated; *P* is the observed height of the splashed funnel; *h* is the water depth; *r* is the radius of explosive charges; R^2 is coefficient of determination; Δ is the value difference of the data around the saturated value.

The general form of the splashed funnel and the compressed zone when blasting concentrated explosive charges with the fluctuation of the water depth and the depth of buried explosive charges in clay from the minimum value to the maximum value which is illustrated in Figure 1.

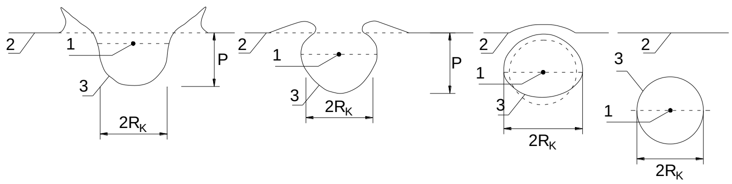

Figure 1. The general form of the splashed funnel and the compressed zone when blasting concentrated explosive charges in submerged clay

1- position of charge in clay; 2- ground surface; 3- funnel or compressed zone

Analyzing the theory system of mechanical effects of the explosion in the ground [5, 6, 7, 8, 10, 11, 13, 14, 16] allowed us making a comment as follows: experiment formulas (11), (12) evolved from the depth of buried explosive charges in clay *W/r* = 11, gradually reached saturated state, means that the domain of smoldered explosion. Hence, it can be executed to orientate the model by adding samples of buried levels *W/r* = 11. It means that when the depth of buried explosive charges in clay *W/r* > 11, we get:

$$\frac{R_K}{r} = \frac{R_{K_{bh}}}{r} \approx 8,\ \text{at}\ \frac{h}{r} > 8 \tag{13}$$

$$\frac{P}{r} = \frac{P_{bh}}{r} = 0,\ \text{at}\ \frac{h}{r} > 24 \tag{14}$$

where P_{bh} is the observed height of splashed funnel when saturated.

Using aforementioned experiment laws above for the range of *h/r* from 0 to 60, *W/r* = 15, 19… allows to present the field of data in three-dimensional space which is demonstrated in Figure 2 and Figure 3. Results of the study denoted that the range of absolute saturation corresponding to values of $\bar{W} \ge 22$, the value of $\bar{R}_K$ was constant at

$\bar{h}$ = 0; and with values of $\bar{W} \geq 28$, the value of $\bar{P}$ = 0 at $\bar{h}$ = 0 [3].

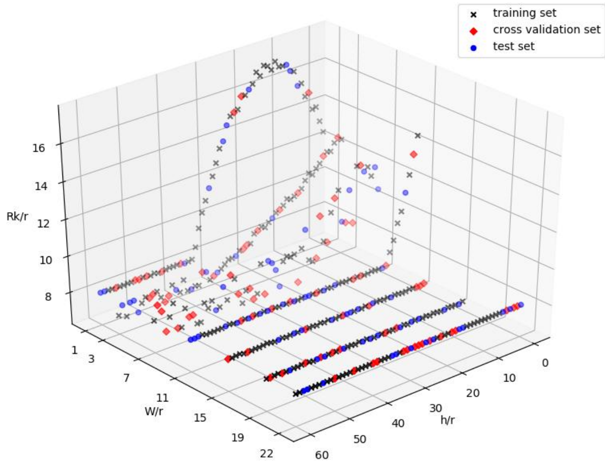

Figure 2. The experiment dependence of the relative radius of the compressed zone $\bar{R}_K$ on the relative water depth $\bar{h}$ and the relative depth of the buried explosive charges $\bar{W}$

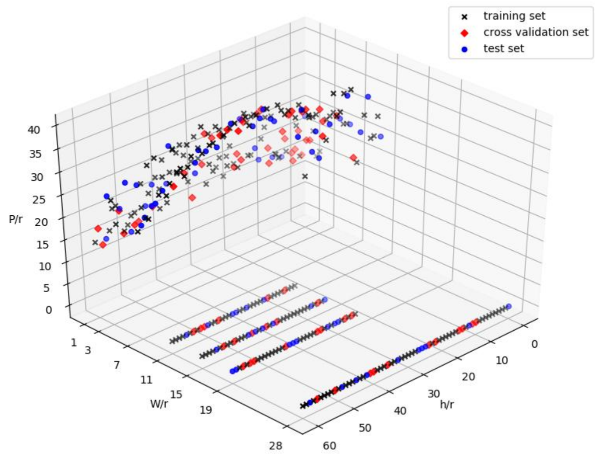

Figure 3. The experiment dependence of the relative radius of the relative observed height of the splashed funnel $\bar{P}$ on the relative water depth $\bar{h}$ and the relative depth of the buried explosive charges $\bar{W}$

2. Theory basis

2.1. Multivariable regression method

Regression is a statistical method analyzing the relation between the dependent variable y and one or more independence variables x_j. Thus, this paper establishes a predicting model, called a hypothesis function $h_{\theta_{(x)}}$ with respect to x_j, with factors are estimation parameters θ_j. This hypothesis function will find out predicting values $\hat{y}$, compared to actual values y. The used loss function in this paper is the mean square error (MSE), estimation parameters θ_j are updated after each epoch, using the entire training set through a technic called "gradient descent". The problem "overfitting" is resolved through hyperparameter λ [18, 19].

Prior to training, data dimensions need to be normalized. Normalizing data dimensions or normalizing variables play an important role in the step of preprocessing data. Normalizing data dimensions is to make the same magnitude of each data dimension. Meanwhile, the relations among data dimensions are kept. Simultaneously, normalizing data dimensions helps each dimension having the same influence on the model, to avoid circumstances where a dimension having the data with high magnitude will affect more efficiently to the model than that of low magnitude. The normalizing procedure which is used in this paper is the standardlisation through expectations μ_j and standard deviations σ_j of each feature, except the feature $x = 1$ [19].

The accuracy of the estimation function (the influence of the model) is evaluated through the coefficient the determination R^2 (R squared). Since R^2 is calculated on the test set after optimizing parameters θ_j on the training set, so the more R^2 comes to 1, the more accuracy of the model gets high.

The data set will be separated into 3 parts: Part 1 – the training set is to train and optimize parameters θ_j; Part 2 – the cross validation set is to find a model with hyperparameters modifying the conformity of the hypothesis function; Part 3 – the test set is to evaluate the efficient of the found model. Three parts of the data set are separated as a ratio of 3:1:1 (it is synonymous that 60%/20%/20%)

If the estimation function just only depends on single independence variables (for example: $x_1, x_2, x_1^2, x_2^2 \ldots$), the relation will not be presented in the case that independence variables x_1, x_2 depend on each other (for example: $x_1.x_2$, $x_1^2.x_2$, $x_1.x_2^2 \ldots$). According to the principle of the blasting influence in an arbitrary medium, the predicting function of the observed height of the splashed funnel or that of the radius of the compressed zone depends on both parameters synthetically: the water depth (x_1) and the depth of buried explosive charges (x_2). Thus, the variable of the water depth and that of the depth of buried explosive charges in clay are just two relative independent variables. Actually, there is a dependence between them through the parameter of the blasting influence zone. Hence, to attain a model having high accuracy, it is needed to combine all probable cases of independence variables in the model corresponding to the degree of hypothesis function. It means that the paper builds 2 nonlinear hypothesis functions corresponding to the estimation of the dependence of $\bar{R}_K$ and $\bar{P}$ on variables $\bar{W}$ and $\bar{h}$.

2.2. Similarity parameters of the blasting influence

To establish the dependence of the radius of the compressed zone R_K, the observed height of the splashed funnel *P* based on parameters such as the depth of buried explosive charges in clay *W*, the water depth *h* and the radius of explosive charges *r*, similarity law is used to make similarity parameters as follows [2, 5, 8, 14]:

- The relative depth of concentrated buried explosive charges is the ratio between the depth of buried explosive charges in clay *W* and the radius of explosive charges *r*: $\bar{W} = W/r$;

- The relative water depth is the ratio between the water depth *h* and the radius of explosive charges *r*: $\bar{h} = h/r$;

- The radius of the relative compressed zone is the ratio between the radius of the compressed zone R_K and the radius of explosive charges *r*: $\bar{R}_K = R_K/r$;

- The relative observed height of the splashed funnel is the ratio between the observed height of the splashed funnel P and the radius of explosive charges *r*: $\bar{P} = P/r$.

3. Analyzing and establishing polynomial regression model

3.1. Determining the radius of the compressed zone

The hypothesis function predicting $\bar{R}_K$ will be built based on the basis of high degree combinations of 2 independent variables $\bar{W}$ and $\bar{h}$. This function has a form:

$$\begin{aligned}\bar{R}_K &= \theta_0 + \theta_1.\frac{h}{r} + \theta_2.\frac{W}{r} + \theta_3.\left(\frac{h}{r}\right)^2 + \theta_3.\frac{h}{r}.\frac{W}{r} + \theta_5.\left(\frac{W}{r}\right)^2 + \ldots + \\ &+ \theta_6.\left(\frac{h}{r}\right)^3 + \theta_7.\left(\frac{h}{r}\right)^2.\frac{W}{r} + \theta_8.\frac{h}{r}.\left(\frac{W}{r}\right)^2 + \theta_9.\left(\frac{W}{r}\right)^3 + \ldots + \\ &+ \sum_{i=1}^{d}\sum_{j=0}^{i}\left\{\left(\frac{h}{r}\right)^{i-j}.\left(\frac{W}{r}\right)^{j}.\theta_{T\,|\,T=\left[\left(\sum_2^d d\right)+1\right]\div\left[\left(\sum_2^d d\right)+1+d\right]}\right\}\end{aligned} \tag{15}$$

where $\bar{R}_K$ is the exchanged radius of the compressed zone; *d* is the degree of estimation function $\bar{R}_K$; θ_0, θ_1, θ_2,… are estimation parameters; $h/r = \bar{h}$ is the exchanged water depth; $W/r = \bar{W}$ is the exchanged depth of buried explosive charges.

If the model of function predicting $\bar{R}_K$ has more than 2 degrees ($d \geq 2$), (15) will be able to be rewritten as follows:

$$\bar{R}_K = \theta_0 + \theta_1.\frac{h}{r} + \theta_2.\frac{W}{r} + \sum_{i=1}^{d}\sum_{j=0}^{i}\left\{\left(\frac{h}{r}\right)^{i-j}.\left(\frac{W}{r}\right)^{j}.\theta_{T\,|\,T=\left[\left(\sum_{2}^{d} d\right)+1\right]\div\left[\left(\sum_{2}^{d} d\right)+1+d\right]}\right\} \,|\, (d \geq 2) \tag{16}$$

The expression (16) can be presented under matrix form as follows:

$$\{\bar{R}_K\} = [X].\{\theta\}$$

where

$$[X] = \left[\{1\}\ \left\{\frac{h}{r}\right\}\ \left\{\frac{W}{r}\right\} \cdots \left\{\frac{h}{r}\right\}^{d} \cdots \left\{\frac{h}{r}\right\}^{i-j} \times \left\{\frac{W}{r}\right\}^{j} \cdots \left\{\frac{W}{r}\right\}^{d}\right] \tag{17}$$

with $[X]$ is matrix $m \times n$ containing column vector elements; *m* is the number of rows of matrix *X* corresponding to training examples; *n* is the number of columns of matrix *X* corresponding to features (variables) of the model, $n = \begin{cases} n_1 = 3 \,|\, d = 1 \\ n_d = n_{d-1} + d + 1 \,|\, d \geq 2 \end{cases}$; *d* is the number of degrees of the model; $\{\theta\}$ is the column vector with the shape of $n \times 1$; $\{\bar{R}_K\}$ is the column vector with the shape of $m \times 1$, the detail as follows:

$$\begin{Bmatrix} \bar{R}_K^{(1)} \\ \bar{R}_K^{(2)} \\ \cdots \\ \bar{R}_K^{(i)} \\ \cdots \\ \bar{R}_K^{(m)} \end{Bmatrix}_{m\times 1} = \begin{bmatrix}
1 & \left(\frac{h}{r}\right)_{(1)} & \left(\frac{W}{r}\right)_{(1)} & \cdots & \left(\frac{h}{r}\right)^{j}_{(1)}\cdots\left(\frac{h}{r}\right)^{j-=1}_{(1)}\left(\frac{W}{r}\right)^{0+=1}_{(1)}\cdots & \left(\frac{W}{r}\right)^{j}_{(1)} & \cdots & \left(\frac{h}{r}\right)^{d}_{(1)}\cdots\left(\frac{h}{r}\right)^{d-=1}_{(1)}\left(\frac{W}{r}\right)^{0+=1}_{(1)}\cdots & \left(\frac{W}{r}\right)^{d}_{(1)} \\
1 & \left(\frac{h}{r}\right)_{(2)} & \left(\frac{W}{r}\right)_{(2)} & \cdots & \left(\frac{h}{r}\right)^{j}_{(2)}\cdots\left(\frac{h}{r}\right)^{j-=1}_{(2)}\left(\frac{W}{r}\right)^{0+=1}_{(2)}\cdots & \left(\frac{W}{r}\right)^{j}_{(2)} & \cdots & \left(\frac{h}{r}\right)^{d}_{(2)}\cdots\left(\frac{h}{r}\right)^{d-=1}_{(2)}\left(\frac{W}{r}\right)^{0+=1}_{(2)}\cdots & \left(\frac{W}{r}\right)^{d}_{(2)} \\
\cdots & \cdots & \cdots & \cdots & \cdots & \cdots & \cdots & \cdots & \cdots \\
1 & \left(\frac{h}{r}\right)_{(i)} & \left(\frac{W}{r}\right)_{(i)} & \cdots & \left(\frac{h}{r}\right)^{j}_{(i)}\cdots\left(\frac{h}{r}\right)^{j-=1}_{(i)}\left(\frac{W}{r}\right)^{0+=1}_{(i)}\cdots & \left(\frac{W}{r}\right)^{j}_{(i)} & \cdots & \left(\frac{h}{r}\right)^{d}_{(i)}\cdots\left(\frac{h}{r}\right)^{d-=1}_{(i)}\left(\frac{W}{r}\right)^{0+=1}_{(i)}\cdots & \left(\frac{W}{r}\right)^{d}_{(i)} \\
\cdots & \cdots & \cdots & \cdots & \cdots & \cdots & \cdots & \cdots & \cdots \\
1 & \left(\frac{h}{r}\right)_{(m)} & \left(\frac{W}{r}\right)_{(m)} & \cdots & \left(\frac{h}{r}\right)^{j}_{(m)}\cdots\left(\frac{h}{r}\right)^{j-=1}_{(m)}\left(\frac{W}{r}\right)^{0+=1}_{(m)}\cdots & \left(\frac{W}{r}\right)^{j}_{(m)} & \cdots & \left(\frac{h}{r}\right)^{d}_{(m)}\cdots\left(\frac{h}{r}\right)^{d-=1}_{(m)}\left(\frac{W}{r}\right)^{0+=1}_{(m)}\cdots & \left(\frac{W}{r}\right)^{d}_{(m)}
\end{bmatrix}_{m\times n} \times \begin{Bmatrix} \theta_0 \\ \theta_1 \\ \cdots \\ \theta_j \\ \cdots \\ \theta_{\left(\sum_{2}^{d} d\right)+1+d} \end{Bmatrix}_{n\times 1} \tag{18}$$

where (1), (2), … , (*i*), …, (*m*) are the orders of samples in the data set (*i* = 1 ÷ *m*); *j* is the degree of the model, *j* = 1 ÷ *d*.

The data set which is employed to establish the predicting model $\bar{R}_K$ has 411 samples, the chosen training set is 247 samples, the cross validation set and the test set are 82 samples/set. To assure that the model is built objectively, the separated ratio will be chosen randomly.

The degree of choice is *d* = 4, calculating errors in both data set of training and cross validation with the gradual increase of λ, the parameter λ is selected so that errors of both training set and cross validation set are the smallest (Figure 4b). Using trial and error method, the case that *d* = 4, λ = 0.1 is the most suitable. The result is shown:

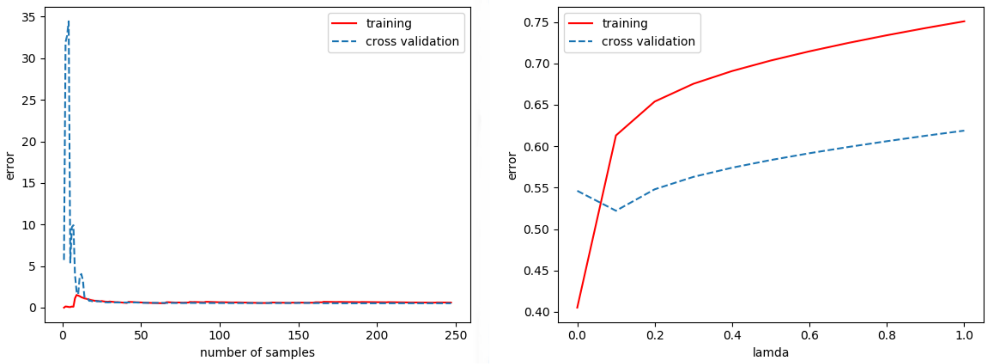

a) *b)*

Figure 4. The error correlation between the training set and the cross validation set with the 4-degree function of the training samples (a), and that of λ (b) when establishing the model $\bar{R}_K$

Due to learning directly from the training set, the model tries to describe its law, so the error in this data set is always low, the result is a blue line in Figure 4a. One set of estimation parameters θ is calculated and adjusted gradually with each increase of the training sample. With each adjustment, θ will be employed to calculate the error of the cross-validation set, the result is an orange line in Figure 4a. The more the vicinity degree between two lines is high, the more the generalization degree of the model is high; the asymptotic level of the two lines is near 0, representing the higher suitability of the model. The result is that both of vicinity degree and zero asymptotic level are high, representing a decent model.

The efficient of the model is evaluated based on the coefficient of determination R^2 with respect to the test set as follows:

$$R^2 = 1 - \frac{\sum_{i=1}^{m}\left(\frac{R_K}{r}^{(i)} - \frac{\hat{R}_K}{r}^{(i)}\right)^2}{\sum_{i=1}^{m}\left(\frac{R_K}{r}^{(i)} - \frac{\bar{R}_K}{r}\right)^2} = 0.825 \tag{19}$$

where $\frac{R_K}{r}^{(i)}$ is the actual value of the radius of the relative compressed zone at the i^{th} blasting in the test set; $\frac{\bar{R}_K}{r}$ is the actual average value of the radius of the relative compressed zone in the test set; $\frac{\hat{R}_K}{r}^{(i)}$ is the predicted value of the radius of the relative compressed zone at the i^{th} blasting which is calculated by the model; m = 82 is the total number of actual samples in the test set.

Parameters building the hypothesis function are shown in Table 1:

Table 1. The hypothesis function form predicting $\bar{R}_K$

θ_j	θ_0	θ_1	θ_2	θ_3	θ_4	θ_5	θ_6	θ_7
	9.03	-1.22	-8.02	-3.60	-1.74	8.52	-0.09	10.76
x_j	1	$\bar{h}$	$\bar{W}$	$\bar{h}^2$	$\bar{h}\ \bar{W}$	$\bar{W}^2$	$\bar{h}^3$	$\bar{h}^2\bar{W}$
μ_j	-	3.09E+01	1.07E+01	1.25E+03	3.45E+02	1.69E+02	5.68E+04	1.42E+04
σ_j	-	1.72E+01	7.45E+00	1.09E+03	3.35E+02	1.71E+02	6.26E+04	1.81E+04
θ_j	θ_8	θ_9	θ_{10}	θ_{11}	θ_{12}	θ_{13}	θ_{14}	-
	1.09	-1.22	2.11	-3.99	-3.81	0.14	-1.65	-
x_j	$\bar{h}\ \bar{W}^2$	$\bar{W}^3$	$\bar{h}^4$	$\bar{h}^3\bar{W}$	$\bar{h}^2\bar{W}^2$	$\bar{h}\ \bar{W}^3$	$\bar{W}^4$	-
μ_j	5.55E+03	3.03E+03	2.75E+06	6.58E+05	2.31E+05	1.00E+05	5.76E+04	-
σ_j	7.02E+03	3.71E+03	3.54E+06	9.86E+05	3.63E+05	1.48E+05	8.06E+04	-

Thus, from (16) and Table 1, the radius of the compressed zone is determined when blasting in the clay medium under water:

$$\frac{R_K}{r} = 9.03 + \frac{-1.22\left(\frac{h}{r} - 30.9\right)}{17.2} + \frac{-8.02\left(\frac{W}{r} - 10.7\right)}{7.45} + \ldots + \frac{-1.65\left(\left(\frac{W}{r}\right)^4 - 5.76\times10^4\right)}{8.06\times10^4}$$

or

$$\frac{R_K}{r} = 9.03 + \sum_{j=1}^{14} \frac{\theta_j \left\{ \left[\left(\frac{h}{r}\right)^{d-=1} . \left(\frac{W}{r}\right)^{d+=1} \right]_{|d=1\div4} - \mu_j \right\}}{\sigma_j} \tag{20}$$

where $j = 1 \div 14$ in Table 1 respectively; θ_j is estimation parameters in Table 1;

μ_j is the expectation or the average value of feature x_j in the training set, $\mu_j = \frac{1}{m}\sum_{i=1}^{m} X_j^{(i)}$;

σ_j is the variance or the standard deviation of feature x_j in the training set, $\sigma_j = \sqrt{\frac{1}{m-1}\sum_{i=1}^{m}\left(x_j^{(i)} - \mu_j\right)^2}$; X_j contains 14 features from the left to the right in Table 1 ($\bar{h}, \bar{W} \ldots \bar{W}^4$); d is the degree of feature x_j, when $d = 1 \div 4$, orderly, the terms in square brackets ([]) in (20) will contain all 14 features of x_j in Table 1; m is the total number of samples in the training set; (i) is the i^{th} element in the training set.

The dependence law of the radius of the compressed zone on the water depth, the depth of buried explosive charges in clay and the radius of explosive charges (20) is shown under dimensionless form in 3-dimension space in Figure 5.

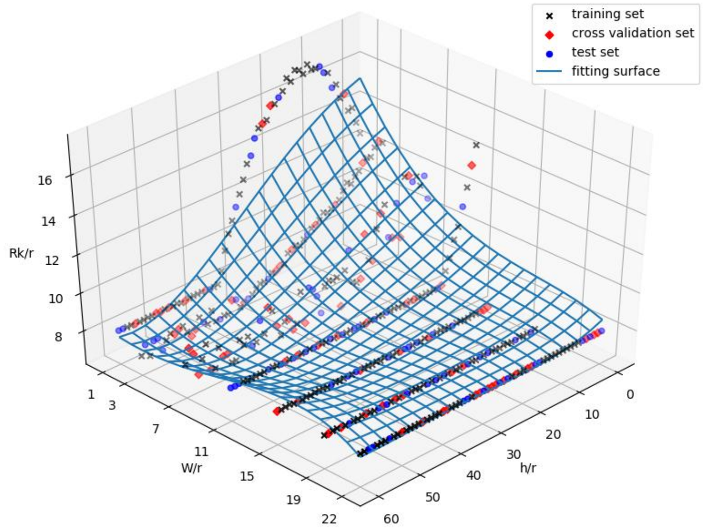

Figure 5. The dependence law of the radius of the compressed zone on the water depth, the depth of buried explosive charges in clay of the chosen model

The result shows that the hypothesis function built from the data reflecting the dependence of the radius of the compressed zone $\bar{R}_K$ on the variables $\bar{W}$ and $\bar{h}$, has relative high accuracy. From Figure 5, a surface consisting of all points calculated in the model is completely able to be employed to predict the radius of the compressed zone $\bar{R}_K$ from all various values of $\bar{W}$ and $\bar{h}$ in the range of the experiment data. However, since the model learns from the data, predicting the interpolation is better than that of the extrapolation. Simultaneously, it is necessary to find out the saturation boundary in experiments orientating the model predicting correctly.

3.2. Determining the observed height of the splashed funnel

Similar to the formation of $\bar{R}_K$, the hypothesis function predicting $\bar{P}$ also has the form as follows:

$$\bar{P} = \theta_0 + \theta_1.\frac{h}{r} + \theta_2.\frac{W}{r} + \sum_{i=1}^{d}\sum_{j=0}^{i}\left\{\left(\frac{h}{r}\right)^{i-j}.\left(\frac{W}{r}\right)^{j}.\theta_{T\,|\,T=\left[\left(\sum_2^d d\right)+1\right]\div\left[\left(\sum_2^d d\right)+1+d\right]}\right\} \mid \left(d \geq 2\right) \qquad (21)$$

where $\bar{P}$ is the exchanged observed height of the splashed funnel; other parameters are similar to that of formula (16).

The data set which is employed to establish the predicting model $\bar{P}$ has 377 samples, the chosen training set is 227 samples, the cross validation set and the test set are 75 samples/set. To assure that the model is built objectively, the separated ratio will be also chosen randomly.

Using the degree of the model $d = 4$, the coefficient of determination R^2 reaches 0.71. Parameters building the hypothesis function are shown in Table 2:

Table 2. The hypothesis function form predicting $\bar{P}$

θ_j	θ_0	θ_1	θ_2	θ_3	θ_4	θ_5	θ_6	θ_7
	13.9	14.21	33.40	-26.67	-49.71	-59.04	27.09	22.33
x_j	1	$\bar{h}$	$\bar{W}$	$\bar{h}^2$	$\bar{h}\ \bar{W}$	$\bar{W}^2$	$\bar{h}^3$	$\bar{h}^2\bar{W}$
μ_j	-	3.28E+01	1.16E+01	1.36E+03	3.88E+02	2.21E+02	6.18E+04	1.64E+04
σ_j	-	1.68E+01	9.34E+00	1.07E+03	3.99E+02	2.81E+02	6.26E+04	2.09E+04
θ_j	θ_8	θ_9	θ_{10}	θ_{11}	θ_{12}	θ_{13}	θ_{14}	-
	0.10	26.05	-15.37	15.57	-33.15	45.34	-8.25	-
x_j	$\bar{h}\ \bar{W}^2$	$\bar{W}^3$	$\bar{h}^4$	$\bar{h}^3\bar{W}$	$\bar{h}^2\bar{W}^2$	$\bar{h}\ \bar{W}^3$	$\bar{W}^4$	-
μ_j	7.32E+03	5.09E+03	2.98E+06	7.61E+05	3.10E+05	1.64E+05	1.28E+05	-
σ_j	1.07E+04	8.06E+03	3.60E+06	1.14E+06	5.35E+05	2.97E+05	2.29E+05	-

Thus, from (21) and Table 2, the observed height of the splashed funnel is determined when blasting in the clay medium under water:

$$\frac{P}{r} = 13.9 + \sum_{j=1}^{14} \frac{\theta_j \left\{ \left[\left(\frac{h}{r}\right)^{d-=1} \cdot \left(\frac{W}{r}\right)^{d+=1} \right]_{|d=1\div 4} - \mu_j \right\}}{\sigma_j} \tag{22}$$

where $j = 1 \div 14$ in Table 2 respectively; θ_j is estimation parameters in Table 2; μ_j, σ_j is the expectation and the variance of features x_j in the training set which are calculated in the same way as formula (20).

The dependence law of $\bar{P}$ on $\bar{W}$ and $\bar{h}$ is shown under dimensionless form in 3-dimension space in Figure 6.

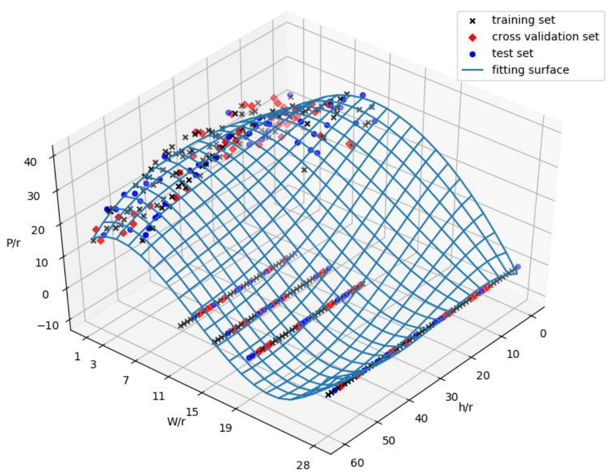

Figure 6. The dependence law of the observed height of the splashed funnel on the water depth, the depth of buried explosive charges in clay of the chosen model

Analyzing the result in Figure 6, it can be seen that the hypothesis function built from the experiment data reflecting the dependence law of the exchanged observed height of the splashed funnel $\bar{P}$ on the variables $\bar{W}$ and $\bar{h}$, has unreasonable accuracy in the range that $\bar{W}$ is greater than or equals to 19. As aforementioned expression (14) above, as well as the study result [2], it was proven that the observed height of the splashed funnel in this region must be 0.

Hence, the formula determining the observed height of the splashed funnel (22), its usage range needs to be restricted where $\bar{W}$ is lower or equals to 19.

Comparing the aforementioned study result above to [2], it can completely make a general comment as follows: values of the observed height of the splashed funnels reach the saturation state (minimum values) when the relative water depth (*h/r*) is about over 26, values of the radius of the compressed zones reach the saturation state (minimum values) when the relative water depth (*h/r*) is about over 36, in all cases that the relative depth of buried explosive charges (*W/r*) in clay is under 11; in the cases that the relative depth of buried explosive charges (*W/r*) in clay is over 11, the radius value of the compressed zone reaches the saturation state when the relative water depth (*h/r*) is greater or equals to 9, the observed height value of the splased funnel reaches the saturation state when the relative water depth (*h/r*) is about greater or equals to 26. It proves that, in the high value of the water depth, the blasting influence in clay will change into the smoldered explosion, which is similar to the on-land blasting.

4. Conclusion, recommendation

Based on the studying result above, some comments can be made as follows:

- When the explosive charges blasting in clay under water, the observed height of the splashed funnel or the radius of the compressed zone depends on 3 parameters: the depth of buried explosive charges, the water depth and the radius of explosive charges.

- The observed height of the splashed funnel or the radius of the compressed zone under water depends increasingly on the radius of explosive charges. If the depth values of buried explosive charges and the water depth values are low enough, the observed height of the splashed funnel or the radius of the compressed zone will depend increasingly on the increase of these values. If the depth values of buried explosive charges and the water depth values are greater, the observed height of the splashed funnel or the radius of the compressed zone will depend decreasingly on the increase of these values. When blasting in the saturation or smoldered explosion, corresponding to the great depth, the observed height of the splashed funnel or the radius of the compressed zone are constants not depending on the depth of buried explosive charges or the water depth.

- The built regression model based on machine learning algorithms which is learned from the data, making a hypothesis function describing the dependence law of the observed height of the splashed funnel, the radius of the compressed zone on the depth of buried explosive charges in clay, the water depth and the radius of explosive charges, in a fairly correct way.

Recommendation: The regression method with a predetermined form of the function has not enough effectiveness in terms of the laws having the high complexity, and high nonlinear rate. In particular, compared to the model of $\bar{R}_K$, the model of $\bar{P}$ has the significant discrete data, the polynomial regression is not decent enough to describe the complexity of this law, so it is necessary to find out another method. For such complex laws, there is an efficient method using deep learning algorithms establishing the model with artificial neural networks, activation functions employed in each layer of a neural network can resolve the extreme nonlinear laws.

References

1. Белин В.А, Дам Чонг Тханг (2006). Экспериментальное исследование линейных донных зарядов выброса для создания каналов и траншей под водой. *Объединенный научный журнал,* No11, Москва, Май.
2. Дам Чонг Тханг., Нгуен Чи Та., Нгуен Тхань Донг (2019). Определения массы сосредоточенного заряда взрывчатого вещества для образования воронки выброса и зоны сжатия камуфлета при взрывании в среде глины под водой. УДК 622.235. “*Взрывное дело*”, No122/79, Издатель ИПКОН РАН, Москва.
3. Дам Чонг Тханг, Белин В.А., Нгуен Тхань Донг (2019). Эмпирические исследования образования воронки выпроса и явления камуфлетта при взрывании сосредоточных зарядов в среде глины под водой. УДК 622.235. “*Взрывное дело*”, No122/79, Издатель ИПКОН РАН, Москва.
4. Галкин В.В., Гильманов Р.А., Дроговейко И.З. (1987). *Взрывные работы под водой*. Недра, Москва.
5. Баум Ф.А., Станюкович К.П., Шехтер Б.И. (1975). *Физика взрыва*. Гасударственное издательство физико-математической литературы, Москва.
6. О.Е. Власов (1957). *Основы терии действия взрыва*. ВИА, Москва.
7. Покровский Г.И., Федоров И.С. (1957). *Действие удара и взрыва в деформируемых средах*, Госстройиздат.
8. Седов Л.И. (1954). *Методы подобия и размерности в механике*, Изд. ГИТЛ.

9. Ромашов. А.Н. (1980). *Особенности действия крупных подземных взрывов*. Недра, Москва.
10. Крюков Г.М. (1985). *Физика взрывного разрушения*. МГИ. Москва.
11. Кутузов Б.Н. (1990). *Лабораторные работы по дисциплине «Разрушение горных пород взрывом»*. МГИ, Москва.
12. Новиков В.Д., Лучко И.А., Юрик И.И., Гляский Г.Я. (1984). *Особенности воронкообразования при подводных взрывах*. Киев, 33с.
13. Городилов Л.В. (1993). *Исследование механического действия взрыва подводных накладных зарядов в грунтах и скальных пород*. Автореферат, Новосибириск.
14. Галкин В.В., Гильманов Р.А., Дроговейко И.З. (1987). *Взрывные работы под водой*. Недра, Москва.
15. Кутузов Б.Н., Рубцов В.К. (1970). *Физика взрывного разрушения горных пород. Раздел 1*. Издательство МГИ. Москва.
16. В.М. Тавривов (1949). *Взрывное дноуглубление*. Издательство министертва речного флота СССР, Москва.
17. Josef Henrych (1979). *The dynamic of explosion and its use*. Academia Prague.
18. Vũ Hữu Tiệp (2018). *Machine learning cơ bản*. Nxb Khoa học và Kỹ thuật.
19. Andrew Ng (2011). *Machine learning online course* at www.coursera.org.

NGHIÊN CỨU THIẾT LẬP SỰ PHỤ THUỘC THỰC NGHIỆM CỦA BÁN KÍNH VÙNG NÉN ÉP VÀ CHIỀU SÂU TRÔNG THẤY CỦA PHỄU NỔ VĂNG TRONG MÔI TRƯỜNG ĐẤT SÉT DƯỚI NƯỚC

Tóm tắt: *Hiện nay, chưa có công thức tổng quát để tính toán cho bán kính vùng nén và chiều sâu trông thấy của phễu nổ phá hủy đất đá dưới nước. Chính vì lý do trên, bài báo đã sử dụng kết quả thực nghiệm nhận được từ nghiên cứu trước trong môi trường đất sét dưới nước và nghiên cứu thiết lập một mô hình hồi quy đa biến để tìm kiếm quy luật thực nghiệm tổng quát về mối liên hệ phụ thuộc của bán kính vùng nén ép và chiều sâu trông thấy của phễu nổ văng trong môi trường sét dưới nước vào chiều sâu nước, chiều sâu tâm nổ trong môi trường đất sét và bán kính lượng nổ. Mô hình được xây dựng với ngôn ngữ lập trình Python 3. Quy luật mô hình lựa chọn được đánh giá, so sánh với giá trị thực tế trong thí nghiệm thông qua hệ số xác định R^2. Kết quả đánh giá cho thấy quy luật lựa chọn có độ chính xác tương đối cao.*

Từ khóa: Nổ; nổ dưới nước; nổ đất sét; nổ văng; nổ nén ép; học máy; hồi quy.

Received: 20/10/2020; *Revised:* 03/12/2020; *Accepted for publication*: 23/12/2020

❑